

# Hovering over a black hole: Entangled fermions in accelerated motion

Benedikt Richter<sup>1,2</sup> and Yasser Omar<sup>1,2,3</sup>

<sup>1</sup>*Physics of Information Group, Instituto de Telecomunicações, Portugal*

<sup>2</sup>*Instituto Superior Técnico, Universidade de Lisboa, Portugal and*

<sup>3</sup>*CEMAPRE, ISEG, Universidade de Lisboa, Portugal*

(Dated: January 31, 2019)

It is well known that the Unruh effect can lead to entanglement degradation when one of the entangled particles is in accelerated motion. Here we study all maximally entangled states of two spinless fermions undergoing (different) accelerations and find that the degradation of entanglement is the same for a wide range of states but, contrary to previous studies where only one of the modes was accelerated, it is not universal. In particular, we identify a class of states for which the loss of quantum correlations is stronger. Furthermore, we discuss the role of fermion statistics and the redistribution of entanglement within the states. Finally, we investigate the case of maximally entangled fermions hovering in the vicinity of the horizon of a Schwarzschild black hole. Although approaching the horizon does degrade the entanglement, we find that it never vanishes: even in the limit where the fermions reach the horizon, the quantum correlations remain available.

PACS numbers: 03.67.Mn, 03.65.-w, 03.65.Ud, 04.62.+v

## I. INTRODUCTION

Quantum theory and general relativity are two well established physical theories that have been tested up to a remarkable precision. Quantum theory describes nature at the very small scales, while general relativity becomes relevant at large macroscopic scales. But still they are not independent and it is expected that gravity, as it constitutes an elementary force, should have a description in terms of a theory of quantum gravity. There is for example the Black Hole Information Paradox [1, 2] whose solution seems to require a theory of quantum gravity. The attempt to restore unitarity in black hole evaporation, combining general relativity and quantum theory, led to a serious tension between these theories [3, 4] that is still to be resolved. An intrinsic feature of quantum theory is the occurrence of entanglement [5] and it is believed that understanding the role of entanglement in black hole evaporation constitutes a major part of the resolution of said paradox. This is one of the main motivations that led to the study of entanglement of particles in non-inertial motion.

It was shown that the presence of an (acceleration) horizon can influence the entanglement of states of quantum fields [6] due to the Unruh effect [7]. In [6] (and also in following work, e.g. [8–15]) maximally entangled states of two modes of non-interacting quantum fields were considered, where one mode was observed by an inertial observer and the other one by a constantly accelerated observer. It was found that entanglement decreases with increasing acceleration until for bosonic fields it finally vanishes [6] and for fermionic fields it approaches a finite value [10]. Especially, the behavior of fermionic fields was studied, e.g. [8–11, 16–18]. But also the creation of entanglement was reported in case one starts from a mixed state [19]. One of the key questions that has been pursued is whether it is possible to carry out quantum information tasks in this relativistic regime [20–

23]. This led to the emergence of the field of relativistic quantum information.

The setting of two accelerated observers was considered for bosonic continuous variable systems in [24, 25]. The tripartite scenario with one inertial and two accelerated observers was analysed, e.g. in [26, 27]. In contrast, here we study maximally entangled states of two modes of a fermionic quantum field, where both modes are observed by accelerated observers. We work in Rindler spacetime and therefore, all our results hold for the general case of two (uniformly) accelerated observers. The widely studied case, we described above, is then recovered by setting the acceleration of one of the observers to zero.

According to the Equivalence Principle, a uniformly accelerated observer experiences the same as an observer that is stationary in a static gravitational field. Thus the general case of two uniformly accelerated observers is equivalent to the description of an entangled state that is stationary in a static gravitational field. Therefore understanding the behavior of entanglement in the setting we are studying here can provide insight into how gravitation effects entanglement. But also on its own the study of entanglement in accelerated frames offers a way to develop a better understanding of the observer dependence of entanglement.

Exploiting the fact that in the near horizon limit the Schwarzschild spacetime approaches two-dimensional Rindler spacetime times a 2-sphere, we are able to describe the consequences hovering over a black hole in the vicinity of the horizon has on a maximally entangled pair of fermionic modes. Then, approaching the horizon corresponds to the limit of infinite acceleration. This is in contrast to previous studies, that considered one inertial and one accelerated observer, i.e. one mode freely falling into a black hole and one mode hovering outside the horizon [16].

In this work we obtain the negativities of all maximally entangled states of two spinless fermionic modes and shed

light on the role of the statistics of the field as well as the finiteness of the surviving entanglement. We observe that entanglement degradation is not universal if both modes are accelerated and study the distribution of entanglement within the states. It is also found that entropy and mutual information are neither universal, but differ for distinct families of states. All these findings contrast with the case of only one accelerated observer. Further, we extend the results to the setting of entangled fermions hovering over an eternal Schwarzschild black hole and compare to the case of one observer falling into the black hole and one observer escaping to fall in, i.e. hovering over the black hole [16].

The outline is the following, in Section II we give a short introduction to quantum field theory in Rindler space. Section III constitutes the main part and is divided into two parts. Part III A is dedicated to the analysis of the degradation of entanglement due to the acceleration experienced by the maximally entangled modes. In III B we calculate the entanglement entropy and further consider the mutual information between the modes as a measure of classical plus quantum correlations. In IV we derive the near horizon limit of the Schwarzschild metric and apply the results to a Schwarzschild black hole. Finally, in V we give the conclusions of this work.

## II. QUANTUM FIELDS IN RINDLER SPACE

We give a brief introduction to quantum field theory in Rindler space. The main purpose is to set up notation and conventions. More details can be found in [11, 28]. We will work in units where  $c = \hbar = k_B = 1$ . Minkowski coordinates  $(t, x)$  and Rindler coordinates  $(\xi, \eta)$  are related by the following transformations

$$t = a^{-1} e^{a\xi} \sinh(a\eta), \quad (1a)$$

$$x = a^{-1} e^{a\xi} \cosh(a\eta), \quad (1b)$$

where in each of the wedges  $-\infty < \xi, \eta < \infty$  and the acceleration is positive  $a > 0$ . Then we obtain the following metric

$$ds^2 = e^{a\xi} (d\eta^2 - d\xi^2) = \rho^2 a^2 d\eta^2 - d\rho^2, \quad (2)$$

where in the second equality we used  $\rho = \frac{1}{a} e^{a\xi}$  and the proper acceleration  $\alpha$  is related to  $a$  by  $ae^{-a\xi} = \alpha$ .

As shown in Figure 1, the two regions  $I$  and  $II$  are causally disconnected due to the presence of horizons at  $x = t$  and  $x = -t$ . A timelike Killing vector in region  $I$  is given by  $\partial_\eta$  ( $-\partial_\eta$  in  $II$ ). We can quantize fields with respect to these Killing vectors independently in the two regions.

We will model the fermionic field by a massless Grassmannian valued scalar field  $\psi$ . Then the quantization of  $\psi$  can be carried out using a complete set of solutions of  $\square\psi = 0$  with support in regions  $I$  and  $II$ , respectively [28]. Therefore the vacuum has the following structure

$$|0\rangle_R = |0\rangle_I \otimes |0\rangle_{II}, \quad (3)$$

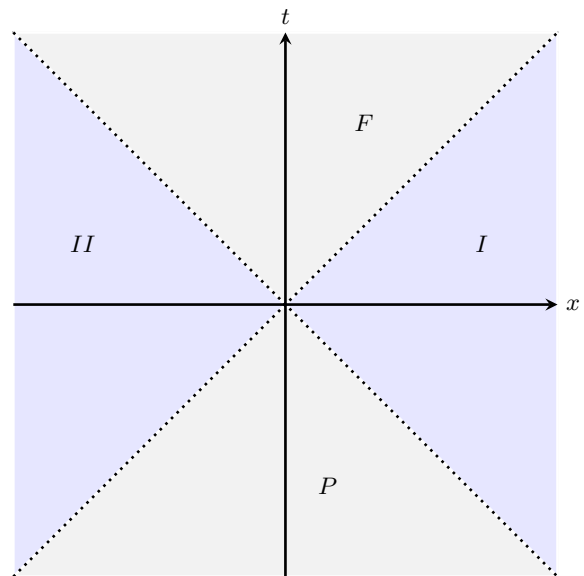


FIG. 1: Rindler space: Regions  $I$  and  $II$  are causally disconnected due to the presence of horizons at  $x = t$  and  $x = -t$ .

where  $|0\rangle_\Gamma = |0\rangle_\Gamma^+ \otimes |0\rangle_\Gamma^-$  ( $\Gamma = I, II$ ) and  $+/-$  denote particles and anti-particles, respectively. In this work we consider accelerated observers confined to Rindler wedge  $I$  and work in the Unruh basis. To obtain the appropriate description of what an accelerated observer is experiencing, we use Bogoliubov transformations to go from the Unruh basis to the Rindler basis. We choose the notation  $|ijkl\rangle_\omega = |i_\omega\rangle_I^+ \otimes |j_\omega\rangle_{II}^- \otimes |k_\omega\rangle_I^- \otimes |l_\omega\rangle_{II}^+$ , where  $+/-$  denote particles and anti-particles, respectively, and obtain for a Unruh mode of energy  $\omega$  and momentum  $k = \omega$  that is initially localized in region  $I$  [11]

$$|0_\omega\rangle_U = \cos^2(r_f)|0000\rangle_\omega - \cos(r_f)\sin(r_f)|0011\rangle_\omega + \cos(r_f)\sin(r_f)|1100\rangle_\omega - \sin^2(r_f)|1111\rangle_\omega, \quad (4a)$$

$$|1_\omega\rangle_U^+ = \cos(r_f)|1000\rangle_\omega - \sin(r_f)|1011\rangle_\omega, \quad (4b)$$

$$|1_\omega\rangle_U^- = \cos(r_f)|0010\rangle_\omega + \sin(r_f)|1110\rangle_\omega, \quad (4c)$$

where the acceleration parameter  $r_f$  is given by  $r_f = \arctan(e^{-\pi\omega/a_\omega})$ . Note that states (4) depend on the acceleration  $a_\omega$  only via the ratio  $\omega/a_\omega$ . Therefore, one observes already at this stage that high frequency modes are less effected by the acceleration  $a_\omega$  as low frequency modes are.

Given a state described by a density matrix  $\rho$  and an accelerated observer that is confined to region  $I$ , we have to trace out the inaccessible region  $II$ . Consider for example the fermionic Minkowski vacuum state  $|0\rangle_M = \prod_\omega |0_\omega\rangle_M = |0\rangle_U$ , then the reduced density matrix  $\rho_I$  is given by

$$\rho_I = \text{Tr}_{II} (|0_\omega\rangle\langle 0_\omega|). \quad (5)$$

Using (4a) it can be seen that this is a thermal state of

temperature  $T_U$  (Unruh temperature) [7]

$$T_U = \frac{a_\omega}{2\pi}. \quad (6)$$

The fermionic partition function  $Z_F^\omega$  can be obtained from (5)

$$Z_F^\omega = 1 + e^{-2\pi\omega/a_\omega} = 1 + e^{-\frac{\omega}{T_U}}. \quad (7)$$

After this preparation we can now move on and study the effects of acceleration on states of maximally entangled fermions.

### III. ENTANGLEMENT AND ENTROPY OF UNIFORMLY ACCELERATED FERMION STATES

Due to the anti-commutativity of fermionic creation/annihilation operators (Pauli Exclusion Principle) there is only a finite number of maximally entangled states of two modes of a fermionic field. Every such state can be obtained from the following set of states  $\{\psi_i\}$  by simple exchanges of particles and anti-particles:

$$|\psi_1\rangle = \frac{1}{\sqrt{2}} (|0_\omega\rangle_U |0_\Omega\rangle_U + |1_\omega\rangle_U^+ |1_\Omega\rangle_U^+) \quad (8a)$$

$$|\psi_2\rangle = \frac{1}{\sqrt{2}} (|1_\omega\rangle_U^- |1_\Omega\rangle_U^- + |1_\omega\rangle_U^+ |1_\Omega\rangle_U^+) \quad (8b)$$

$$|\psi_3\rangle = \frac{1}{\sqrt{2}} (|1_\omega\rangle_U^+ |1_\Omega\rangle_U^- + |1_\omega\rangle_U^- |1_\Omega\rangle_U^+) \quad (8c)$$

$$|\psi_4\rangle = \frac{1}{\sqrt{2}} (|1_\omega\rangle_U^+ |0_\Omega\rangle_U + |1_\omega\rangle_U^- |1_\Omega\rangle_U^+) \quad (8d)$$

$$|\psi_5\rangle = \frac{1}{\sqrt{2}} (|1_\omega\rangle_U^+ |0_\Omega\rangle_U + |0_\omega\rangle_U |1_\Omega\rangle_U^+) \quad (8e)$$

We have chosen one representative of each family; e.g. the states  $\frac{1}{\sqrt{2}} (|1_\omega\rangle_U^- |0_\Omega\rangle_U + |0_\omega\rangle_U |1_\Omega\rangle_U^\pm)$  show the same behavior as  $\psi_5$ . The subscript  $U$  emphasizes that we are

working in the Unruh basis. We ignore here the possibility of a relative phase, as it could be absorbed in a local transformation and thus does not affect entanglement. Therefore, by studying states (8), we obtain the negativities of all maximally entangled states.

#### A. Negativity

We consider two fermionic modes  $\omega$  and  $\Omega$  undergoing constant accelerations  $a_\omega$  and  $a_\Omega$ . The acceleration parameters of the modes are denoted by  $r_f^\omega$  and  $r_f^\Omega$ , respectively. Therefore, starting from states  $\{\psi_i\}$  written in the Unruh basis we use (4) to obtain the density matrices  $\rho_{I,II}^{(i)}$

$$\rho_{I,II}^{(i)} = |\psi_i\rangle\langle\psi_i|. \quad (9)$$

To describe the system as it is seen by an observer confined to region  $I$ , we have to trace out modes that have their support in the inaccessible region. Then the reduced density matrix  $\rho_i$  is given by

$$\rho_i = \text{Tr}_{II} \left( \rho_{I,II}^{(i)} \right). \quad (10)$$

As a measure of entanglement we use the negativity  $N$  that is an entanglement monotone [29]. The negativity for a composite system (we denote the subsystems by  $A$  and  $B$ ) described by a density matrix  $\rho = \rho_{AB}$  is given by the sum of the absolute values of the negative eigenvalues of the partially transposed density matrix  $\rho_{AB}^{pT}$

$$N = \frac{1}{2} \sum_j (|\lambda_j| - \lambda_j), \quad (11)$$

where the  $\lambda_j$ 's are the eigenvalues of  $\rho_{AB}^{pT}$ . So to obtain the negativities  $N_i$  of states  $\psi_i$ , we have to calculate the partially transposed reduced density matrices  $\rho_i^{pT}$ . We find that these matrices are block diagonal. More details of the calculations can be found in Appendix A. The final results for the negativities read

$$N_{i=1,2,3,4} = \frac{1}{2} \cos^2(r_f^\omega) \cos^2(r_f^\Omega), \quad (12)$$

$$N_5 = \frac{1}{4} \left( \sqrt{\left( \sin^2(r_f^\omega) + \sin^2(r_f^\Omega) \right)^2 + 4 \cos^2(r_f^\omega) \cos^2(r_f^\Omega)} - \left( \sin^2(r_f^\omega) + \sin^2(r_f^\Omega) \right) \right). \quad (13)$$

Having obtained the analytic expressions for the negativities of all maximally entangled fermion states, we see that the negativities of the majority of states can be given in form of a simple expression. For two observers with

different accelerations we obtain

$$N_i = \frac{1}{2} \frac{1}{Z_F^\omega} \frac{1}{Z_F^\Omega}, \quad (14)$$

where  $i$  runs from 1 to 4,  $T_{\omega/\Omega}$  are the Unruh temperatures (6) corresponding to the respective accelerations  $a_\omega$

and  $a_\Omega$ ,  $Z_F^{\omega/\Omega}$  the partition function (7) and  $\omega$ ,  $\Omega$  are the energies of the modes. Considering states  $\{\psi_i\}_{i=1,2,3,4}$  it is interesting to note that

$$N_{i=1,2,3,4}(r_f^\omega, r_f^\Omega) = 2N_f(r_f^\omega)N_f(r_f^\Omega), \quad (15)$$

where we denoted  $N_{i=1,2,3,4}(r_f^\omega, r_f^\Omega = 0)$  by  $N_f(r_f^\omega)$ . Note that  $N_f(r_f^\omega)$  is the negativity in case of only one mode being seen by an accelerated observer (acceleration parameter  $r_f^\omega$ ). The negativity  $N_f(r_f^\omega) = \frac{1}{2} \cos^2(r_f^\omega)$  was obtained, for example, in [10]. This product structure is absent for state  $\psi_5$ , where the negativity is given by

$$N_5 = \frac{1}{2} \left( \sqrt{\frac{1}{Z_F^\omega} \frac{1}{Z_F^\Omega} + \frac{1}{4} (n_F^\omega + n_F^\Omega)^2} - \frac{1}{2} (n_F^\omega + n_F^\Omega) \right), \quad (16)$$

where we introduced the occupation numbers  $n_F^\omega = (1 + e^{\omega/T_\omega})^{-1}$  and  $n_F^\Omega = (1 + e^{\Omega/T_\Omega})^{-1}$ . Thus, the degradation of entanglement in the case of a fermionic field shows universal behavior for a wide range of possible maximally entangled states. But there is one family of states,  $\psi_5$ , for which entanglement is less robust against acceleration, see Figure 2.

There is a fundamental difference between states  $\psi_{i=1,2,3,4}$  and  $\psi_5$ . While each state  $\psi_i$  is a superposition of two states of the form  $|k_\omega\rangle_U |l_\Omega\rangle_U$  ( $k, l \in \{0, 1^+, 1^-\}$ ), only for state  $\psi_5$  both such states lead to a contribution to a (the same) diagonal element of the reduced density matrix that is relevant for entanglement. More precisely, for non-vanishing acceleration,  $|1_\omega\rangle_U^+ |0_\Omega\rangle_U$  as well as  $|0_\omega\rangle_U |1_\Omega\rangle_U^+$  contribute to the matrix element  $|1_\omega\rangle_U^+ |1_\Omega\rangle_U^+ \langle 1_\omega|_U^+ \langle 1_\Omega|_U^+$  of the reduced density matrix. This is well reflected in the expression for the negativity, given by (16). The contribution of  $|1_\omega\rangle_U^+ |0_\Omega\rangle_U$  is quantified by  $n_F^\Omega$  and the one of  $|0_\omega\rangle_U |1_\Omega\rangle_U^+$  by  $n_F^\omega$ . Due to the symmetry, (16) depends only the average occupation number  $\bar{n}_F = 1/2(n_F^\omega + n_F^\Omega)$ . This behavior distinguishes  $\psi_5$  from the other  $\psi_i$ .

As in the setting of one mode seen by an accelerated observer and one mode seen by an inertial observer [10, 11, 17], in the limit of infinite acceleration the negativity does not vanish, but approaches a finite limit. The surviving entanglement is calculated to be

$$\lim_{r_f^\omega, r_f^\Omega \rightarrow \infty} N_{i=1,2,3,4} = \frac{1}{8}, \quad (17a)$$

$$\lim_{r_f^\omega, r_f^\Omega \rightarrow \infty} N_5 = \frac{1}{4} (\sqrt{2} - 1). \quad (17b)$$

The fact that there is entanglement surviving in this limit is specific for initially pure maximally entangled states and contrasts with the case of starting from a tripartite state, where one observer is inertial and two observers are accelerated. In that case, after tracing out the inertial observer, the bipartite entanglement between the modes observed by accelerated observers vanishes in this limit

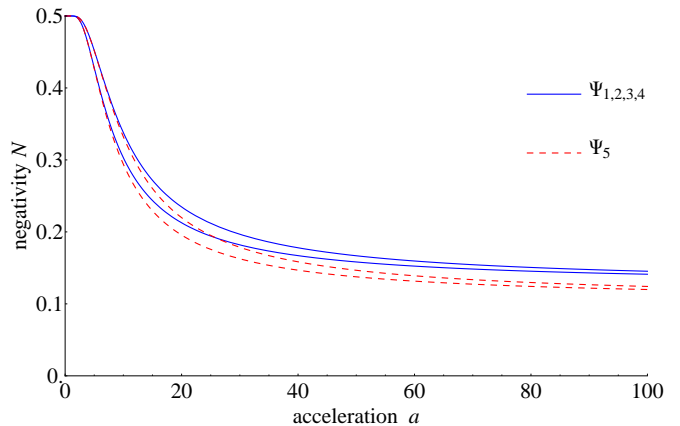


FIG. 2: Negativities for maximally entangled fermion states  $\{\psi_i\}$  versus acceleration  $a = a_\omega = a_\Omega$  for  $\omega = 2$ ,  $\Omega = 2$  (bottom pair of curves) and  $\omega = 2$ ,  $\Omega = 3$  (top pair of curves). States  $\{\psi_i\}_{i=1,2,3,4}$  show identical behavior regarding degradation of entanglement (blue, continuous), whereas the negativity of  $\psi_5$  degrades faster (red, dashed). The finite asymptotic values for states  $\{\psi_i\}_{i=1,2,3,4}$  and  $\psi_5$  are  $1/8$  and  $1/4(\sqrt{2} - 1)$ , respectively. Further we see that entanglement of modes of higher energy is more robust for finite acceleration.

[27]. Numerical studies of fermionic mixed state entanglement also showed that entanglement is extinguished for most states in the infinite acceleration limit [30].

Our results reduce to the known results for one accelerated observer if one takes the limit  $r_f^\Omega \rightarrow 0$  and we obtain the universal behavior reported in [10]

$$\lim_{r_f^\Omega \rightarrow 0} N_{i=1,2,\dots,5} \equiv N_f = \frac{1}{2} \cos^2(r_f^\omega) \quad (18)$$

and thus

$$\lim_{r_f^\omega \rightarrow \infty} N_f = \frac{1}{4}. \quad (19)$$

To summarize, there is no universality in the degradation of entanglement for maximally entangled fermion states if both modes are seen by accelerated observers. That is a feature that was absent in previous studies of one accelerated observer. Furthermore, it can be seen from (17) that there is less surviving entanglement in the case of two accelerated observers. For states  $\{\psi_i\}_{i=1,2,3,4}$  the negativity approaches exactly one half of the limiting value of  $N_f$ , while the entanglement in  $\psi_5$  is degraded even further. We want to emphasize that all the  $N_i$  can be expressed in terms of the fermion partition function  $Z_F$  and the fermion occupation number  $n_F$ . These quantities are characteristics of the statistics of the underlying field (fermionic or bosonic) and thus the effects of statistics are manifest in the expressions of the  $N_i$ . Then the physical reason for the non-vanishing of entanglement in

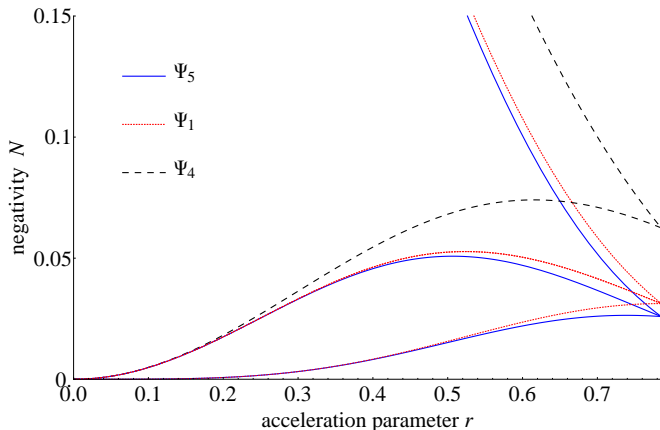


FIG. 3: Entanglement distribution for states  $\psi_1$  (red, dotted),  $\psi_4$  (black, dashed) and  $\psi_5$  (blue) plotted versus the acceleration parameter  $r = r_f^\omega = r_f^\Omega$ . The infinite acceleration limit corresponds to  $r = \frac{\pi}{4}$ . The middle pair of solid curves is twofold degenerate due to the symmetry of the states. With increasing acceleration, entanglement is created in previously separable sectors. From top to bottom the curves correspond to: red:  $N(0, 0 | 1^+, 1^+)$ ,  $N(1^-, 0 | 1^+ 1^-, 1^+)$  and  $N(0, 1^- | 1^+, 1^+ 1^-)$ ,  $N(1^-, 1^- | 1^+ 1^-, 1^+ 1^-)$ ; blue:  $N(1^+, 0 | 0, 1^+)$ ,  $N(1^+ 1^-, 0 | 1^-, 1^+)$  and  $N(1^+, 1^- | 0, 1^+ 1^-)$ ,  $N(1^+ 1^-, 1^- | 1^-, 1^+ 1^-)$ ; black:  $N(1^+, 0 | 1^-, 1^+)$ ,  $N(1^+, 1^- | 1^-, 1^+ 1^-)$

initially maximally entangled fermion states is given by the finiteness of the fermionic partition function  $Z_F$ , that is due to the small number of states allowed by fermion statistics and by the Pauli Exclusion Principle. Acceleration “just causes rotations” in the initial states.

The consequence of the fact that states (4) depend on the acceleration  $a_\omega/\Omega$  only via the ratios  $\omega/a_\omega$  and  $\Omega/a_\Omega$ , are manifest in Figure 2. One observes that high frequency modes are less effected by acceleration than low frequency modes are. This is due to the larger wavelength of low energy modes. The larger the wavelength, and therefore the spatial extension, compared to the inverse Unruh temperature, the more the system gets “stretched” by the acceleration. Thus the effects of acceleration are stronger in this case and the rate of entanglement degradation is higher.

Interestingly, the behavior of the negativity under acceleration does not depend on whether there is entanglement created in some sectors or not. We define a sector of a state  $\psi_i$  as follows: A sector of state  $\psi_i$  consists of all the elements of the reduced density matrix  $\rho_i$  that contribute to one block of the block diagonal partially transposed reduced density matrix  $\rho_i^{pT}$ . For example,  $\psi_1$  has four sectors, as can be seen from the partially transposed reduced density matrix  $\rho_1^{pT}$  (see (A1) in Appendix A). When the acceleration is increasing from zero, entanglement decreases in the sector where it is initiated and, depending

on the particular structure of the state, entanglement is created in previously non-entangled sectors. For states  $\psi_1$ ,  $\psi_4$  and  $\psi_5$  we observe creation of entanglement in some sectors, while there is no entanglement production for  $\psi_2$  and  $\psi_3$  (see Appendix A 2 for more details). We plot the entanglement in the sectors that show creation of entanglement in Figure 3. This effect is due to a symmetric production of particle-antiparticle pairs. We can, for example, write state  $\psi_1$  schematically as  $0, 0 | 1^+, 1^+$ . Then, for non-zero acceleration, the Unruh effect, that in some sense can be seen as pair production, populates states  $0, 1^-$  and  $1^+, 1^+ 1^-$  and thus creates entanglement ( $N(0, 1^- | 1^+, 1^+ 1^-) \neq 0$ ) in the sector  $0, 1^- | 1^+, 1^+ 1^-$ . In the same manner there is entanglement created in the sectors  $1^-, 0 | 1^+ 1^-, 1^+$  and  $1^-, 1^- | 1^+ 1^-, 1^+ 1^-$ , see Figure 3. The reason why there is no entanglement generated for  $\psi_2$  and  $\psi_3$  is that for these states symmetric pair production would require a violation of the Pauli Principle and therefore is forbidden.

After this detailed study of the negativity of states (8), we now move on to analyse the entropy and the mutual information of these states. This provides further insight into the effects acceleration has on the correlations in fermion states.

## B. Entropy and mutual information

In this Section we analyse entropy and mutual information of the fermion states. Since we are considering accelerated observers and therefore trace out region  $II$  to obtain the reduced density matrices  $\rho_i$ , the resulting state is not pure any more. Thus, the entropy of  $\psi_i$  increases due to entanglement with modes in region  $II$ . Among the different measures of entropy, the most widely used is the von Neumann entropy  $S$ , given by

$$S(\rho_i) = -Tr_I(\rho_i \log(\rho_i)). \quad (20)$$

Usually the von Neumann entropy  $S$  is hard to calculate and so sometimes the Rényi-2 entropy  $S_2$  is used instead. In our setting, the von Neumann entropy can be calculated analytically. Since the corresponding expressions are quite long and not very enlightening, we give the plots of  $S$  as a function of the acceleration in Figure 4. In the limit of infinite acceleration the von Neumann entropies approach the asymptotic values  $S^\infty(\rho_i)$ , that are

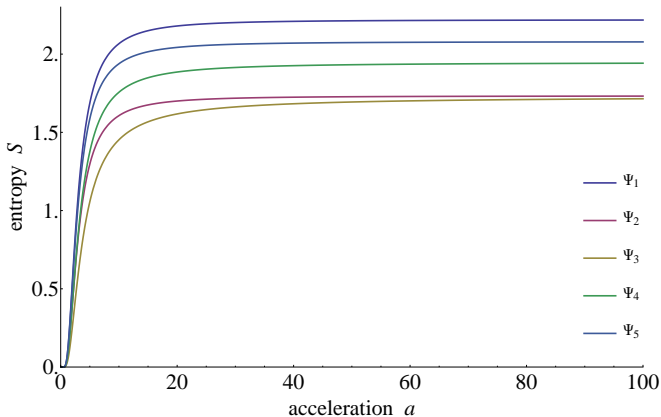


FIG. 4: von Neumann entropies of maximally entangled fermion states  $\{\psi_i\}$  versus acceleration  $a = a_\omega = a_\Omega$  for frequencies  $\omega = \Omega = 1$ . From bottom to top:  $\psi_3, \psi_2, \psi_4, \psi_5, \psi_1$ . The entanglement of states  $\{\psi_i\}$  with modes in region  $II$  increases with acceleration and approaches its finite asymptotic value.

given in the following

$$S^\infty(\rho_1) = \frac{\log(32)}{4} - \frac{3 + 2\sqrt{2}}{8} \log\left(\frac{3 + 2\sqrt{2}}{32}\right) + \frac{2\sqrt{2} - 3}{8} \log\left(\frac{3 - 2\sqrt{2}}{32}\right), \quad (21a)$$

$$S^\infty(\rho_2) = S^\infty(\rho_3) = \frac{\log(32)}{2}, \quad (21b)$$

$$S^\infty(\rho_4) = \log\left(\frac{16}{3^{3/4}}\right), \quad (21c)$$

$$S^\infty(\rho_5) = \log(8). \quad (21d)$$

The Rényi-2 entropy  $S_2$  is given by the formula

$$S_2(\rho_i) = -\log(\text{Tr}_I \rho_i^2). \quad (22)$$

For more details, including the analytical expressions of  $S_2$ , see Appendix B.

Furthermore, we calculate the mutual information  $I$  between modes  $\omega$  and  $\Omega$  as a measure of quantum and classical correlations as

$$I_i = S(\text{Tr}_\omega(\rho_i)) + S(\text{Tr}_\Omega(\rho_i)) - S(\rho_i), \quad (23)$$

where  $\text{Tr}_{\omega/\Omega}$  denotes the trace over mode  $\omega/\Omega$ . The resulting mutual information of states  $\{\psi_i\}_{i=1,2,\dots,5}$  is shown in Figure 5. In the limit of infinite acceleration the surviving correlations are given by  $I_i^\infty$ :

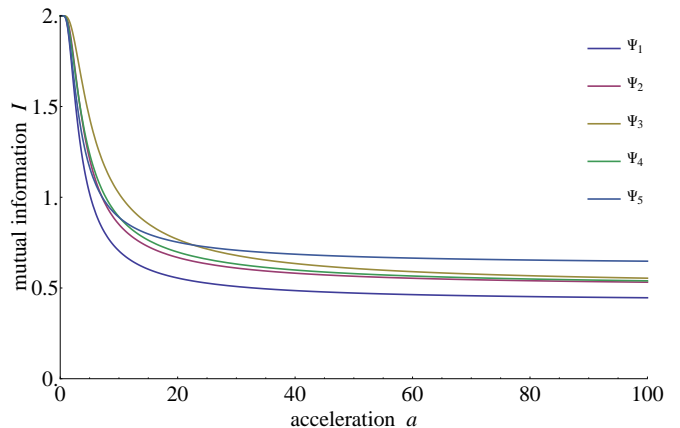


FIG. 5: Mutual information, measured in bits, for maximally entangled fermion states  $\{\psi_i\}$  plotted versus acceleration  $a = a_\omega = a_\Omega$  for frequencies  $\omega = \Omega = 1$ . From bottom to top:  $\psi_1, \psi_2, \psi_4, \psi_3, \psi_5$ . The mutual information of states  $\psi_{i=2,3,4}$  approaches 0.5 while for states  $\psi_1$  this value is about 0.4 and for the state  $\psi_5$  it is approximately 0.6.

$$I_1^\infty = \frac{1}{8 \log(2)} \left( -\log\left(\frac{531441}{256}\right) + (3 + 2\sqrt{2}) \log(3 + 2\sqrt{2}) + (3 - 2\sqrt{2}) \log(3 - 2\sqrt{2}) \right), \quad (24a)$$

$$I_2^\infty = I_3^\infty = I_4^\infty = \frac{1}{2}, \quad (24b)$$

$$I_5^\infty = -\log\left(\frac{3\sqrt{3}}{8}\right) / \log(2). \quad (24c)$$

In Section III A we saw that the negativities of states  $\{\psi_i\}_{i=1,2,3,4}$  are equal, while the negativity of state  $\psi_5$  degraded faster with increasing acceleration. None of the states becomes separable for any acceleration. Here we analysed the mutual information of these states as a further measure of correlations between the modes and found that there are three distinct limiting cases (24). First, there are states  $\psi_2, \psi_3$  and  $\psi_4$ , for which  $I^\infty = 1/2$ . Since  $I$  measures classical and quantum correlations, and the negativity of these state approaches one quarter of its initial value in the infinite acceleration limit, we suspect that classical and quantum correlations are degraded equally, i.e.  $I^0 = I_{cl}^0 + I_{qu}^0 = 1 + 1 \rightarrow 1/4 + 1/4$ , where  $I^0$  denotes the initial mutual information between the modes. Further, there are states  $\psi_1$  that show less correlation in the infinite acceleration limit  $I^\infty \approx 0.4$  and states  $\psi_5$ , that remain most correlated  $I^\infty \approx 0.6$ . We conclude that, in all cases, also classical correlations become degraded with increasing acceleration.

As it can be seen from Figure 4, the entanglement entropies vanish for zero acceleration, as the global state is pure. So there is no entanglement between states  $\psi_i$  and

modes in region  $II$ . As the acceleration increases, an acceleration horizon forms and entanglement increases due to tracing out modes with support in the region behind the horizon. In contrast to the negativities of the states, the entropy is different for each state for all finite accelerations. Note that, except for states  $\psi_2$  and  $\psi_3$ , the infinite acceleration limits are also distinct. So we see that the entanglement between modes in the accessible region and modes in the inaccessible region does not increase equally for all states, but depends strongly on the particular  $\psi_i$ .

In this Section we studied the degradation of quantum and classical correlations in fermion states that is caused by uniform acceleration. In the following Section we will extend these results to the case of entangled fermions hovering over a Schwarzschild black hole.

#### IV. ENTANGLED FERMIONS HOVERING OVER A BLACK HOLE

In the presence of a Schwarzschild black hole the spacetime outside the black hole is characterized by the Schwarzschild metric

$$ds^2 = \left(1 - \frac{R_S}{r}\right) dt^2 - \frac{1}{1 - \frac{R_S}{r}} dr^2 - r^2 d\Omega^2, \quad (25)$$

where  $G$  is the gravitational constant,  $M$  is the mass of the black hole,  $R_S = 2GM$  is the Schwarzschild radius and  $d\Omega^2$  is the line element of the unit 2-sphere. In order to obtain the limiting form of (25) close to the horizon of a Schwarzschild black hole, we consider an observer placed at  $r = r_0$  with proper time  $\eta = (1 - 2GM/r_0)t$ . Introducing

$$\rho^2 = 8GM(r - 2GM), \quad (26)$$

we obtain the following metric up to terms of order  $\frac{1}{2GM}$  in the near horizon limit

$$ds^2 = ds_R^2 - ds_2^2, \quad (27)$$

where

$$ds_R^2 = \frac{1}{16G^2M^2} \left(1 - \frac{2GM}{r_0}\right)^{-1} \rho^2 d\eta^2 - d\rho^2, \quad (28)$$

$$ds_2^2 = (2GM)^2 d\Omega^2. \quad (29)$$

So (25) reduces to the product of two-dimensional Rindler space ( $ds_R^2$ ) and a 2-sphere of radius  $2GM$  ( $ds_2^2$ ). Comparing  $ds_R^2$  to the two-dimensional Rindler metric (2) we see that the acceleration  $a$  experienced by an observer at fixed position  $r = r_0$  is given by

$$a = \frac{1}{4GM} \left(1 - \frac{2GM}{r_0}\right)^{-\frac{1}{2}}. \quad (30)$$

To extend the considerations of Section III in 2d Rindler space to this spacetime, we consider the wave

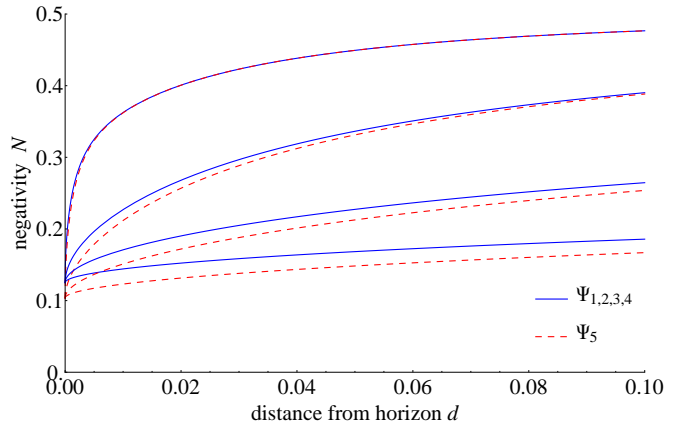


FIG. 6: Negativities for maximally entangled fermion states  $\{\psi_i\}$  close to a Schwarzschild black hole as functions of the distance  $d$  from the horizon (measured in units of  $R_S$ ). States  $\{\psi_i\}_{i=1,2,3,4}$  show identical behavior regarding degradation of entanglement (blue, continuous), whereas the negativity of  $\psi_5$  degrades faster (red, dashed). From top to bottom the curves show the four cases  $\omega_g = 10$  and  $\Omega_g = 50$ ,  $\omega_g = 5$  and  $\Omega_g = 10$ ,  $\omega_g = 2$  and  $\Omega_g = 5$ ,  $\omega_g = 1$  and  $\Omega_g = 2$ . So the entanglement of modes of higher energies degrades closer to the horizon.

equation for a massless scalar field  $\psi$  that is given by  $\square\psi = 0$ . In the near horizon limit (27) we can write

$$(\square_R - \Delta_{S^2})\psi(\eta, \rho, \phi, \theta) = 0, \quad (31)$$

where  $\phi, \theta$  are angular coordinates,  $\square_R$  is the d'Alembertian of 2d Rindler space and  $\Delta_{S^2}$  is the Laplacian of the 2-sphere. We are looking for solutions of the form

$$\psi(\eta, \rho, \phi, \theta) = \psi_{rad}(\eta, \rho)\psi(\phi, \theta)_{ang}, \quad (32)$$

that satisfy

$$\square_R\psi_{rad}(\eta, \rho) = 0, \quad (33)$$

$$\Delta_{S^2}\psi_{ang}(\phi, \theta) = 0. \quad (34)$$

The solutions of (33) are the well known solutions of the Klein Gordon equation in Rindler space that we used above. The eigenfunctions of  $\Delta_{S^2}$  are given by the spherical harmonics  $Y_l^m(\phi, \theta)$ . The eigenvalues are  $l(l+1)$ . So we pick the eigenfunctions with  $l = 0$ , i.e.

$$\psi_{ang}(\phi, \theta) = e^{im\phi} P_{l=0}^m(\cos(\theta)) = 1, \quad (35)$$

where the  $P_l^m(\cos(\theta))$  are the associated Legendre polynomials. We conclude that for the choice  $l = 0$ , i.e. zero angular momentum, we can describe the near horizon limit by restricting our considerations to 2d Rindler space.

Therefore, in the following we restrict ourselves to wave functions  $\psi$  of vanishing angular momentum satisfying

(32). We consider maximally entangled fermion states (8) to hover over a black hole at some distance  $d = r_0 - R_S$  from the horizon. Then the system can be described in 2d Rindler space (for some more details on this correspondence see [16]). The analogue of the Rindler vacuum  $|0\rangle_I$  is the Boulware vacuum  $|0\rangle_B$  and the Unruh vacuum  $|0\rangle_U$  corresponds to the Hartle-Hawking vacuum  $|0\rangle_H$ . Further, the physical effect that causes the degradation of entanglement is now the Hawking effect. So, using results from III, we can reveal the fading of correlations near the horizon. Near to a black hole of mass  $M$  the acceleration  $a$  in (2) is set by (30). So, we see that the limit of infinite acceleration corresponds to the limit of  $r_0$  approaching  $R_S$ . As in [16] we introduce the rescaled frequencies  $\omega_g$  and  $\Omega_g$  as

$$\omega_g = 4\pi R_S \omega. \quad (36)$$

To see at which distance  $d$  from the horizon the degradation of entanglement actually happens, we plot the negativity for different frequencies against the distance from the horizon in Figure 6. We see that fermions stay entangled even near the black hole horizon, even in the limit of being at the horizon. The surviving negativity in the horizon limit was obtained in (17) and is finite. The same is not true for mixed states, which are non-maximally entangled. In this case there is in general no entanglement surviving [27, 30].

The qualitative behavior regarding entanglement degradation is similar to the case of one mode hovering over the black hole and one mode is freely falling in [16]. One difference is that the negativities are always smaller in the case considered here. The crucial point that distinguishes two hovering modes from the case of an infalling mode and one that hovers outside the horizon is that in this case there is no universality among the maximally entangled states. States  $\psi_5$  keep substantially less entanglement, where for finite distances from the horizon the difference between the negativities is largest for low frequency modes (see Figure 6). Setting the acceleration parameter of one of the modes to zero, we recover the results of [16]. Finally we want to mention that although the approximation of the Schwarzschild spacetime by Rindler spacetime times a 2-sphere is only valid at small distances from the horizon, i.e. as long as the following condition holds [16]

$$\frac{r - R_S}{R_S} \ll 1, \quad (37)$$

it seems that the degradation of entanglement becomes significant for low frequency modes at remarkably large distances from the horizon (of the order  $\approx R_S$ ).

As the negativities, also the mutual information (23) between the modes of the fermion states does not show an universal behavior and we see that when approaching the black hole horizon the mutual information between the modes decreases at different rates for each of the states. Finally, in the limit of reaching the horizon we can classify the states according to the remaining correlations in

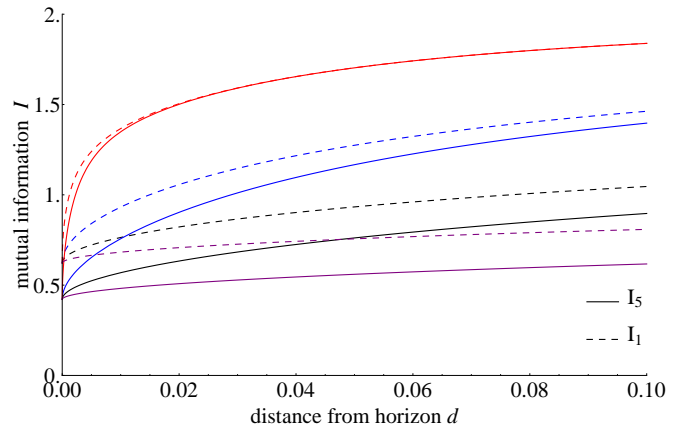


FIG. 7: Mutual information, measured in bits, for maximally entangled fermion states  $\{\psi_i\}$  near the horizon as function of the distance  $d$  from the horizon (measured in units of  $R_S$ ).  $I_5$  (continuous) and  $I_1$  (dashed) decrease close to the black hole horizon and approach finite values. From top to bottom the (pairs of) curves show the four cases  $\omega_g = 10$  and  $\Omega_g = 50$ ,  $\omega_g = 5$  and  $\Omega_g = 10$ ,  $\omega_g = 2$  and  $\Omega_g = 5$ ,  $\omega_g = 1$  and  $\Omega_g = 2$ . The higher the energy of the modes the closer to the horizon the correlations become degraded.

three classes, where  $\psi_5$  is the most and  $\psi_1$  the least correlated in this limit. For better visibility we plot only the mutual information of states  $\psi_1$  and  $\psi_5$  that bound the mutual information of the remaining states from below and above, respectively, in Figure 7. Similarly to the degradation of the negativities (Figure 6), higher energy modes remain more correlated even close to the black hole horizon until, in the limit of reaching the horizon, the common (state-dependent) limiting value is approached. Furthermore, the difference between the amount of correlations present in the states is largest for low energy modes, while for modes of higher energy the differences are small. Note that, for all states, classical correlations are degraded as well as quantum correlations. The entanglement of states (8) with modes in the inaccessible region of the eternal black hole, as measured by the entanglement entropy (20) or (22), heavily depends on the particular state.

In the case of one observer falling into a black hole and one hovering outside, it was suggested in [10] that the remaining entanglement is purely from fermionic statistics, i.e. there is some entanglement in the initial state that cannot be removed. The main argument was the universality of entanglement degradation that was found in [10]. Further, it was also shown that a violation of the CHSH inequality is not possible using these states when local operations and classical communication (LOCC) are not allowed [31, 32]. Here we found no universality and so, along the same lines, one could argue this hints that the surviving entanglement goes beyond purely fermionic sta-

tistical correlations (at least for some of the states). In this case, it would seem that when one mode is crossing the horizon freely falling, quantum correlations that are potentially useful are deleted, while they remain available when both fermions hover outside the horizon. Furthermore, it is worth mentioning that LOCC are allowed in this region of spacetime and that, in general, fermionic statistics can be used as a resource for quantum information tasks [33–35]. This interesting point deserves further investigation that is beyond the scope of this work.

Here we treated the black hole classically, without applying any particular model of quantum gravity. One might be concerned about the validity of this procedure. But as we saw, the degradation of correlations occurs at distances large compared to  $L_P$  (Planck length) and therefore working in the classical background is justified.

## V. CONCLUSIONS

In this work we studied maximally entangled states of a fermionic quantum field in uniform acceleration. For all fermionic states of two maximally entangled modes we analysed the correlations when both modes are (differently) accelerated. This extends previous work that usually considered one accelerated mode entangled with a mode in inertial motion.

One point that caused discussions in the past is the role played by the statistics of the field (fermionic or bosonic) in the degradation of entanglement due to acceleration, e.g. [12, 14]. We obtained analytical expressions for the negativities in terms of the fermion partition function and the occupation numbers. This sheds light on the importance of the statistics of the particular field, as these quantities reflect its statistical properties. In particular, the finite value of the surviving entanglement for fermions can be understood by the finiteness of the fermion partition function.

Previously, it was shown that in the case of one accelerated observer the negativity of a wide range of states is given by  $N_f$  (cf. (18)), i.e. it is universal [10]. We found that the same is true for the majority of states ( $\{\psi_i\}_{i=1,2,3,4}$ ) considered here. Furthermore, we found that for these states we can express the negativity  $N$  as

$$N = 2 N_f(r_f^\omega) N_f(r_f^\Omega). \quad (38)$$

That is, the negativities of the uniformly accelerated fermion states are given by the product of the negativities of the case of one accelerated and one inertial observer. But interestingly there is one class of states,  $\psi_5$ , that shows a quantitatively different behavior. The rate of decrease of entanglement is higher than for the other classes, and even the surviving entanglement in the infinite acceleration limit is less. Comparing to the case of one accelerated mode [10], we see that entanglement is degraded further by a factor of 2. Still all maximally entangled fermion states are entangled for all accelerations, and the minimum negativity across all states is

given by  $\frac{1}{4}(\sqrt{2} - 1) \approx 0.1$ . This is in contrast to the behavior of most fermionic mixed states [27, 30] and bosons in a maximally entangled state, where entanglement is completely lost in the infinite acceleration limit [24, 25]. Furthermore, we analysed the creation of entanglement in various sectors of states  $\psi_i$ , and described the role the structure of the states plays in this phenomenon. We found that only a subset of states admits a structure that is compatible with the creation of entanglement in one or more sectors.

We found that also classical correlations are partially lost due to acceleration. The mutual information monotonically decreases with increasing acceleration and approaches distinct state-dependent values in the infinite acceleration limit. Therefore also the degradation of classical correlations depends on the particular state. We want to emphasize that the state-dependence of the asymptotic mutual information is absent in the case of one accelerated observer, as in this case the asymptotic value is 1. This can be explained by the fact that there is essentially no difference between, for example,  $\psi_1$  and  $\psi_5$  states when just one mode is seen by an accelerated observer.

Furthermore, we found that the entanglement entropy, and therefore the entanglement with modes in the inaccessible region, depend on the particular kind of maximally entangled state. This shows that the correlations between the two regions are state-dependent.

Restricting to the case of zero angular momentum states, we were able to study maximally entangled fermions hovering over a Schwarzschild black hole. As in the scenario of one mode freely falling into a black hole and the other mode hovering outside [16], there is entanglement surviving even when the horizon is approached. The most distinguishing feature between these cases is the non-universality of entanglement degradation, that we found among the fermion states. Furthermore, we obtained that also the degradation of classical correlations differs in both cases.

It is worth to mention that the degradation of correlations between two fermions depends heavily on the energy of the modes. While correlations in states of low energy are degraded already at relatively large distances from the black hole horizon, the degradation of correlations in high energy states takes place in the close vicinity of the horizon.

Finally, based on the universality of entanglement degradation in the case of one infalling mode and one mode hovering outside the horizon, it was suspected that the surviving correlations are due to fermion statistics [10]. We found that, in the case of two fermions hovering over a black hole, entanglement degradation is not universal, and so it seems reasonable that, even in the limit of reaching the horizon, (at least some) states contain surviving quantum correlations that are not only from fermionic origin.

## ACKNOWLEDGMENTS

We would like to thank Dieter Lüst for useful discussions. Further we thank the support from Fundação para a Ciência e a Tecnologia (Portugal), namely through programmes PTDC/POPH and projects PEst-OE/EGE/UI0491/2013, PEst-OE/EEI/LA0008/2013, UID/EEA/50008/2013, IT/QuSim and CRUP-CPU/CQVibes, partially funded by EU FEDER, and from the EU FP7 projects LANDAUER (GA 318287) and PAPETS (GA 323901). BR acknowledges the support from the DP-PMI and FCT (Portugal) through scholarship SFRH/BD/52651/2014.

## Appendix A: Negativities

### 1. Calculation of negativities

We give more details of the calculations of the negativities of the fermion states. The calculation of the negativity (11) requires the partially transposed reduced density matrices  $\rho_i^{pT}$  of states (8). We obtain the density matrices according to (9) and by tracing out region  $II$  we end up with the reduced density matrices of the fermion states  $\rho_i$ . Finally, by partial transposition (let  $\rho = \sum_{ijkl} p_{ijkl} |i\rangle\langle j| \otimes |k\rangle\langle l|$  then  $\rho^{pT} = \sum_{ijkl} p_{ijkl} |i\rangle\langle j| \otimes |l\rangle\langle k|$  is the partial transposed) we obtain the  $\rho_i^{pT}$ . These are block diagonal. In case of state  $\psi_1$  the part of  $\rho_1^{pT}$  that gives rise to negative eigenvalues is of the following form

$$\begin{pmatrix} 1 & 0 & 0 & 0 \\ 0 & \tan^2(r_f^\omega) & 0 & 0 \\ 0 & 0 & \tan^2(r_f^\Omega) & 0 \\ 0 & 0 & 0 & \tan^2(r_f^\omega) \tan^2(r_f^\Omega) \end{pmatrix} \otimes \rho_{(1)}^{pT}, \quad (\text{A1})$$

where  $\otimes$  denotes the Kronecker product and

$$\rho_{(1)}^{pT} = \frac{1}{2} \cos^2(r_f^\omega) \cos^2(r_f^\Omega) \times \begin{pmatrix} \sin^2(r_f^\omega) \cos^2(r_f^\Omega) & \cos(r_f^\omega) \cos(r_f^\Omega) \\ \cos(r_f^\omega) \cos(r_f^\Omega) & \sin^2(r_f^\Omega) \cos^2(r_f^\omega) \end{pmatrix}. \quad (\text{A2})$$

Calculating the negative eigenvalues of (A1) the negativity  $N_1$  can be expressed as

$$\begin{aligned} N_1 &= (1 + \tan^2(r_f^\omega) + \tan^2(r_f^\Omega) + \tan^2(r_f^\omega) \tan^2(r_f^\Omega)) \times \\ &\quad \times N(\rho_{(1)}^{pT}) \\ &= \frac{1}{2} \cos^2(r_f^\omega) \cos^2(r_f^\Omega). \end{aligned} \quad (\text{A3})$$

In case of state  $\psi_2$  the part of  $\rho_2^{pT}$  that gives rise to negative eigenvalues is given by

$$\frac{1}{2} \cos^2(r_f^\omega) \cos^2(r_f^\Omega) \begin{pmatrix} 0 & 1 \\ 1 & 0 \end{pmatrix}. \quad (\text{A4})$$

With this result we can again calculate the negativity  $N_2$  and obtain the same result

$$N_2 = \frac{1}{2} \cos^2(r_f^\omega) \cos^2(r_f^\Omega). \quad (\text{A5})$$

State  $\psi_3$  behaves similar under acceleration and we obtain the part of  $\rho_3^{pT}$  that gives rise to negative eigenvalues to be

$$\frac{1}{2} \cos^2(r_f^\omega) \cos^2(r_f^\Omega) \begin{pmatrix} 0 & 1 \\ 1 & 0 \end{pmatrix}. \quad (\text{A6})$$

With this result we can calculate the negativity  $N_3$  to be

$$N_3 = \frac{1}{2} \cos^2(r_f^\omega) \cos^2(r_f^\Omega). \quad (\text{A7})$$

In case of state  $\psi_4$  the part of  $\rho_4^{pT}$  that gives rise to negative eigenvalues is of the form

$$\begin{pmatrix} 1 & 0 \\ 0 & \tan^2(r_f^\Omega) \end{pmatrix} \otimes \rho_{(4)}^{pT}, \quad (\text{A8})$$

where

$$\rho_{(4)}^{pT} = \frac{1}{2} \cos^2(r_f^\omega) \cos^2(r_f^\Omega) \begin{pmatrix} 0 & \cos(r_f^\Omega) \\ \cos(r_f^\Omega) & \sin^2(r_f^\Omega) \end{pmatrix}. \quad (\text{A9})$$

Again the negativity  $N_4$  is calculated to be

$$N_4 = \frac{1}{2} \cos^2(r_f^\omega) \cos^2(r_f^\Omega). \quad (\text{A10})$$

As we saw, state  $\psi_5$  is special. The part of  $\rho_5^{pT}$  that gives rise to negative eigenvalues is of the same form as (A1), but this time  $\rho_{(i)}^{pT}$  is of different structure. There is one element, that has the form of a sum of contributions of the two different modes.  $\rho_{(5)}^{pT}$  is given by

$$\begin{aligned} \rho_{(5)}^{pT} &= \frac{1}{2} \cos^2(r_f^\omega) \cos^2(r_f^\Omega) \\ &\quad \times \begin{pmatrix} 0 & \cos(r_f^\omega) \cos(r_f^\Omega) \\ \cos(r_f^\omega) \cos(r_f^\Omega) & \sin^2(r_f^\omega) + \sin^2(r_f^\Omega) \end{pmatrix} \end{aligned} \quad (\text{A11})$$

and  $N_5$  is

$$\begin{aligned} N_5 &= (1 + \tan^2(r_f^\omega) + \tan^2(r_f^\Omega) + \tan^2(r_f^\omega) \tan^2(r_f^\Omega)) \times \\ &\quad \times N(\rho_{(5)}^{pT}) \\ &= \frac{1}{4} \left( \sqrt{(\sin^2(r_f^\omega) + \sin^2(r_f^\Omega))^2 + 4 \cos^2(r_f^\omega) \cos^2(r_f^\Omega)} \right. \\ &\quad \left. - (\sin^2(r_f^\omega) + \sin^2(r_f^\Omega)) \right). \end{aligned} \quad (\text{A12})$$

### 2. Entanglement in different sectors

We briefly discuss the distribution of entanglement in states  $\psi_i$ , when the acceleration is non-vanishing. Considering (A1) we see that, while entanglement in the sector where it was initiated is decreasing with increasing

acceleration, there is entanglement created in previously non-entangled sectors. Schematically we can write  $N_1$  as

$$\begin{aligned} N_1 = & N(0, 0 | 1^+, 1^+) \\ & + N(1^-, 0 | 1^+ 1^-, 1^+) \\ & + N(0, 1^- | 1^+, 1^+ 1^-) \\ & + N(1^-, 1^- | 1^+ 1^-, 1^+ 1^-), \end{aligned} \quad (\text{A13})$$

where

$$N(0, 0 | 1^+, 1^+) = N(\rho_{(1)}^{pT}), \quad (\text{A14})$$

$$N(1^-, 0 | 1^+ 1^-, 1^+) = \tan^2(r_f^\omega) N(\rho_{(1)}^{pT}), \quad (\text{A15})$$

$$N(0, 1^- | 1^+, 1^+ 1^-) = \tan^2(r_f^\Omega) N(\rho_{(1)}^{pT}), \quad (\text{A16})$$

$$N(1^-, 1^- | 1^+ 1^-, 1^+ 1^-) = \tan^2(r_f^\omega) \tan^2(r_f^\Omega) N(\rho_{(1)}^{pT}) \quad (\text{A17})$$

are the negativities of the different sectors.  $N(0, 0 | 1^+, 1^+)$  is the negativity of the sector, where the entanglement is initialized, i.e. entanglement between  $|0_\omega\rangle_I^+ \otimes |0_\omega\rangle_I^- \otimes |0_\Omega\rangle_I^+ \otimes |0_\Omega\rangle_I^-$  and  $|1_\omega\rangle_I^+ \otimes |0_\omega\rangle_I^- \otimes |1_\Omega\rangle_I^+ \otimes |0_\Omega\rangle_I^-$ . There are three sectors in which entanglement is created due to acceleration (A15)-(A17). The negativities are plotted in Figure 3 and we see that the entanglement is distributed equally between the sectors in the infinite acceleration limit.

In case of states  $\psi_2$  and  $\psi_3$  there is no entanglement created in any sector (cf. (A4) and (A6)) and only the sector, that is initially entangled contributes to the negativity.

Considering state  $\psi_4$  we see from (A8) that there is entanglement created in one previously non-entangled sector. Namely, we can write  $N_4$  schematically as

$$\begin{aligned} N_4 = & N(1^+, 0 | 1^-, 1^+) \\ & + N(1^+, 1^- | 1^-, 1^+ 1^-), \end{aligned} \quad (\text{A18})$$

where

$$N(1^+, 0 | 1^-, 1^+) = N(\rho_{(4)}^{pT}), \quad (\text{A19})$$

$$N(1^+, 1^- | 1^-, 1^+ 1^-) = \tan^2(r_f^\Omega) N(\rho_{(4)}^{pT}), \quad (\text{A20})$$

while  $N(1^+, 0 | 1^-, 1^+)$  is decreasing from its initial value  $1/2$ ,  $N(1^+, 1^- | 1^-, 1^+ 1^-)$  is increasing monotonically. For state  $\psi_5$  we see again, that entanglement is created in some sectors and we can write  $N_5$  schematically as

$$\begin{aligned} N_5 = & N(1^+, 0 | 0, 1^+) \\ & + N(1^+ 1^-, 0 | 1^-, 1^+) \\ & + N(1^+, 1^- | 0, 1^+ 1^-) \\ & + N(1^+ 1^-, 1^- | 1^-, 1^+ 1^-), \end{aligned} \quad (\text{A21})$$

where

$$N(1^+, 0 | 0, 1^+) = N(\rho_{(5)}^{pT}), \quad (\text{A22})$$

$$N(1^+ 1^-, 0 | 1^-, 1^+) = \tan^2(r_f^\omega) N(\rho_{(5)}^{pT}), \quad (\text{A23})$$

$$N(1^+, 1^- | 0, 1^+ 1^-) = \tan^2(r_f^\Omega) N(\rho_{(5)}^{pT}), \quad (\text{A24})$$

$$N(1^+ 1^-, 1^- | 1^-, 1^+ 1^-) = \tan^2(r_f^\omega) \tan^2(r_f^\Omega) N(\rho_{(5)}^{pT}) \quad (\text{A25})$$

are the negativities of the different sectors.  $N(1^+, 0 | 0, 1^+)$  is the negativity of the sector, where the entanglement is initialized. When the acceleration increases from zero the negativity  $N(1^+, 0 | 0, 1^+)$  decreases while (A23)-(A25) increase. In the infinite acceleration limit all sectors are equally entangled, see Figure 3. Comparing states  $\psi_1$  and  $\psi_5$ , we note that the ‘‘redistribution’’ of entanglement is identical for small accelerations, but differs more and more with increasing acceleration, until finally different limiting values are approached. As discussed in III, the creation of entanglement is due to the creation of particle-antiparticle pairs, where the particle is localized in region  $II$  and the antiparticle in region  $I$ .

## Appendix B: Rényi-2 entropies

The Rényi-2 entropies (22) are given in the following (see Figure 8). For convenience we carry out the calculations for  $r^\omega = r^\Omega = r$ . Due to the relative simplicity, we are able to find compact analytical expressions for the Rényi-2 entropies of states (8)

$$S_2(\rho_1) = -\log\left(\frac{(20 \cos(4r) + \cos(8r) + 43)^2}{4096}\right), \quad (\text{B1a})$$

$$S_2(\rho_2) = -\log\left(\sin^8(r) + \frac{1}{16} \sin^4(2r) + \cos^8(r)\right), \quad (\text{B1b})$$

$$S_2(\rho_3) = -\log\left(\frac{3}{2} \sin^8(r) + \frac{1}{32} \sin^4(2r) + \cos^8(r)\right), \quad (\text{B1c})$$

$$\begin{aligned} S_2(\rho_4) = & -\log\left(\frac{1}{1024}(-124 \cos(2r) + 495 \cos(4r) + \right. \\ & \left. -6 \cos(6r) + 42 \cos(8r) + 2 \cos(10r) + \right. \\ & \left. + \cos(12r) + 614)\right), \end{aligned} \quad (\text{B1d})$$

$$S_2(\rho_5) = -3 \log(\sin^4(r) + \cos^4(r)) \quad (\text{B1e})$$

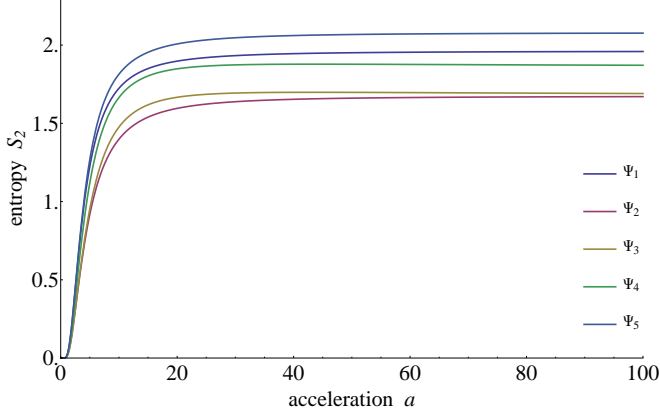


FIG. 8: Rényi-2 entropy for maximally entangled fermion states  $\{\psi_i\}$  plotted versus acceleration  $a = a_\omega = a_\Omega$  for frequencies  $\omega = \Omega = 1$ . From bottom to top:  $\psi_2, \psi_3, \psi_4, \psi_1, \psi_5$ . For state  $\psi_5$  the asymptotic values of  $S$  and  $S_2$  coincide.

and we find the infinite acceleration limits

$$S_2^\infty(\rho_1) = \log\left(\frac{64}{9}\right), \quad (\text{B2a})$$

$$S_2^\infty(\rho_2) = S_2^\infty(\rho_3) = \log\left(\frac{16}{3}\right), \quad (\text{B2b})$$

$$S_2^\infty(\rho_4) = \log\left(\frac{32}{5}\right), \quad (\text{B2c})$$

$$S_2^\infty(\rho_5) = \log(8). \quad (\text{B2d})$$

- 
- [1] S. W. Hawking, *Commun. Math. Phys.* **43**, 199 (1975).  
[2] S. W. Hawking, *Phys. Rev. D* **14**, 2460 (1976).  
[3] S. L. Braunstein, S. Pirandola, and K. Życzkowski, *Phys. Rev. Lett.* **110**, 101301 (2013).  
[4] A. Almheiri, D. Marolf, J. Polchinski, and J. Sully, *J. High Energy Phys.* **2013**, 1 (2013).  
[5] E. Schrödinger, *Naturwissenschaften* **23**, 823 (1935).  
[6] I. Fuentes-Schuller and R. B. Mann, *Phys. Rev. Lett.* **95**, 120404 (2005).  
[7] W. G. Unruh, *Phys. Rev. D* **14**, 870 (1976).  
[8] P. M. Alsing, I. Fuentes-Schuller, R. B. Mann, and T. E. Tessier, *Phys. Rev. A* **74**, 032326 (2006).  
[9] Q. Pan and J. Jing, *Phys. Rev. A* **77**, 024302 (2008).  
[10] E. Martín-Martínez and J. León, *Phys. Rev. A* **80**, 042318 (2009).  
[11] D. E. Bruschi, J. Louko, E. Martín-Martínez, A. Dragan, and I. Fuentes, *Phys. Rev. A* **82**, 042332 (2010).  
[12] E. Martín-Martínez and I. Fuentes, *Phys. Rev. A* **83**, 052306 (2011).  
[13] Q. Pan and J. Jing, *Phys. Rev. D* **78**, 065015 (2008).  
[14] E. Martín-Martínez and J. León, *Phys. Rev. A* **81**, 032320 (2010).  
[15] D. E. Bruschi, A. Dragan, I. Fuentes, and J. Louko, *Phys. Rev. D* **86**, 025026 (2012).  
[16] E. Martín-Martínez, L. J. Garay, and J. León, *Phys. Rev. D* **82**, 064006 (2010).  
[17] J. León and E. Martín-Martínez, *Phys. Rev. A* **80**, 012314 (2009).  
[18] S. Khan, N. A. Khan, and M. Khan, *Commun. Theor. Phys.* **61**, 281 (2014).  
[19] M. Montero and E. Martín-Martínez, *J. High Energy Phys.* **2011**, 1 (2011).  
[20] D. E. Bruschi, A. Dragan, A. R. Lee, I. Fuentes, and J. Louko, *Phys. Rev. Lett.* **111**, 090504 (2013).  
[21] E. Martín-Martínez, D. Aasen, and A. Kempf, *Phys. Rev. Lett.* **110**, 160501 (2013).  
[22] N. Friis, D. E. Bruschi, J. Louko, and I. Fuentes, *Phys. Rev. D* **85**, 081701 (2012).  
[23] K. Brádler, P. Hayden, and P. Panangaden, *J. High Energy Phys.* **2009**, 074 (2009).  
[24] G. Adesso, I. Fuentes-Schuller, and M. Ericsson, *Phys. Rev. A* **76**, 062112 (2007).  
[25] G. Adesso, S. Ragy, and D. Girolami, *Class. Quant. Grav.* **29**, 224002 (2012).  
[26] J. Wang and J. Jing, *Phys. Rev. A* **83**, 022314 (2011).  
[27] M. Shamirzaie, B. N. Esfahani, and M. Soltani, *Int. J. Theor. Phys.* **51**, 787 (2012).  
[28] N. D. Birrell and P. C. W. Davies, *Quantum fields in curved space*, 7 (Cambridge university press, 1984).  
[29] G. Vidal and R. F. Werner, *Phys. Rev. A* **65**, 032314 (2002).  
[30] M. Montero, J. León, and E. Martín-Martínez, *Phys. Rev. A* **84**, 042320 (2011).  
[31] N. Friis, P. Köhler, E. Martín-Martínez, and R. A. Bertlmann, *Phys. Rev. A* **84**, 062111 (2011).  
[32] A. Smith and R. B. Mann, *Phys. Rev. A* **86**, 012306 (2012).  
[33] S. Bose, A. Ekert, Y. Omar, N. Paunković, and V. Vedral, *Phys. Rev. A* **68**, 052309 (2003).  
[34] N. Paunković, Y. Omar, S. Bose, and V. Vedral, *Phys. Rev. Lett.* **88**, 187903 (2002).  
[35] Y. Omar, N. Paunković, S. Bose, and V. Vedral, *Phys. Rev. A* **65**, 062305 (2002).